Mixed active metabolites of the SNP-6 series of novel compounds mitigate metabolic dysfunction-associated steatohepatitis and fibrosis: promising results from pre-clinical and clinical trials

Hsin-Tien Ho[1], Yu-Lueng Shih[2], Tien-Yu Huang[2], Wen-Hui Fang[3], Chang-Hsien Liu[4,5,6], Jung-Chun Lin[2], Chih-Weim Hsiang[4], Kai-Min Chu[1], Cheng-Huei Hsiong[1], Guan-Ju Chen[1], Yung-En Wu[1], Jia-Yu Hao[1], Chih-Wen Liang[1] and Oliver Yoa-Pu Hu[7,8]*

Abstract

Background Metabolic dysfunction-associated steatohepatitis (MASH) is a growing global health concern with no effective pharmacological treatments. SNP-630, a newly developed synthetic molecule with multiple mechanisms of action, and a mixture of two of its active metabolites (SNP-630-MS) inhibit CYP2E1 expression to prevent reactive oxygen species generation, thereby reducing the accumulation of hepatic triglycerides and lowering chemokine levels. This study investigated the SNP-630's potential to alleviate the liver injury in MASH and its efficacy in both a mouse model and patients with MASH to identify a drug candidate that targets multiple pathways implicated in MASH.

Methods SNP-630 and SNP-630-MS were separately administered to the MASH mouse model. The tolerability, safety, and efficacy of SNP-630-MS were also evaluated in 35 patients with MASH. The primary endpoint of the study was assessment of the changes in serum alanine aminotransferase (ALT) levels from baseline to week 12, while the secondary endpoints included the evaluation of liver inflammation, steatosis, and fibrosis parameters and markers.

Results SNP-630 treatment in mice improved inflammation, liver steatosis, and fibrosis compared with that in the MASH control group. Both SNP-630 and SNP-630-MS treatments markedly reduced ALT levels, hepatic triglyceride content, and the expression of inflammatory cytokines monocyte chemoattractant protein 1 and fibrotic collagen (i.e., *Col1a1, Col3a1,* and *Timp1*) in mice. In the clinical trial, patients treated with SNP-630-MS exhibited significant improvement in ALT levels at week 12 compared with baseline levels, with no reports of severe adverse events. This improvement in ALT levels surpassed that achieved with most other MASH candidates. SNP-630-MS demonstrated potential antifibrotic effects, as evidenced by a significant decrease in the levels of fibrogenesis-related biomarkers such as CCL4, CCL5, and caspase 3. Subgroup analysis using FibroScan measurements further indicated the efficacy of SNP-630-MS in ameliorating liver fibrosis.

*Correspondence:
Oliver Yoa-Pu Hu
hyp@tmu.edu.tw
Full list of author information is available at the end of the article

Ho *et al. Journal of Translational Medicine*   (2024) 22:936

Page 2 of 18

Conclusions SNP-630 and SNP-630-MS demonstrated favorable results in mice. SNP-630-MS showed excellent tolerability in mice and patients with MASH. Efficacy analyses indicated that SNP-630-MS improved liver steatosis and injury in patients with MASH, suggesting that SNP-630 and 630-MS are promising therapeutic options for MASH. Larger scale clinical trials remain warranted to assess the efficacy and safety of SNP-630 in MASH.

Trial registration: ClinicalTrials.gov NCT03868566. Registered 06 March 2019-Retrospectively registered, https://clinicaltrials.gov/study/NCT03868566

Keywords Metabolic dysfunction-associated steatohepatitis, SNP-630, Alanine aminotransferase

Background

Metabolic dysfunction-associated steatohepatitis (MASH), also known as non-alcoholic steatohepatitis (NASH), is an advanced stage of metabolic dysfunction-associated steatotic liver disease (MASLD), formerly known as non-alcoholic fatty liver disease (NAFLD) characterized by the accumulation of lipids in liver cells along with inflammation and subsequent fibrosis [1]. MASH can progress to severe conditions such as cirrhosis and hepatocellular carcinoma, posing life-threatening risks. It has been projected that by 2030, the prevalence of MASLD among adults will reach 33.5% [2]. Despite numerous studies conducted to understand the causes of MASLD, no approved pharmacotherapies are currently available [3, 4]. Consequently, there remains an urgent need to identify potential molecular targets for effective treatment by investigating the underlying mechanisms involved in the progression of MASH.

The underlying molecular pathogenesis of MASLD/MASH is complex and has been considered a "multiple-hit" process, which involves multiple parallel factors acting synergistically on the liver and leading to the development or progression of the disease [5]. Therefore, evolving therapeutic targets for MASH has been categorized into four major groups: (1) metabolic targets that reduce insulin resistance, inhibit key enzymes involved in de novo lipogenesis (DNL), or enhance mitochondrial fatty acid β-oxidation [5, 6]; (2) inflammation targets that focus on blocking inflammatory cell infiltration (i.e., macrophage and CD8 T lymphocyte), suppressing inflammatory pathways (i.e., blocking Toll-like receptor 4 or TLR4 signaling), preventing oxidative damage induced by ER stress, or inhibiting hepatocyte cell death [7–9]; (3) gut-liver axis targets that involve modulating the enterohepatic circulation of bile acids, modifying the gut microbiome or lowering lipopolysaccharide (LPS) level [10]; and (4) anti-fibrotic targets that directly act on hepatic stellate cells, reduce collagen synthesis, assembly and deposition, or enhance fibrolysis in the liver [11–13]. Given the multifaceted nature of MASH progression, targeting a single pathway or molecule may not be sufficient [14–16]. There is a growing interest in exploring combination therapies that can simultaneously address different targets involved in the underlying pathogenesis of the disease.

One of the key events in the development of MASLD is insulin resistance, which increases hepatic DNL and impairs the inhibition of adipocyte lipolysis. Together with elevated free fatty acid (FFA) levels in serum, the accumulation of FFA within the hepatocyte increases, which results in steatosis. Ongoing accumulation of FFA leads to endoplasmic reticulum (ER) stress and mitochondrial dysfunction, which induce excessive oxidative stress [17, 18].

Oxidative stress is a major contributor to liver injury and the progression of MASLD, primarily driven by the excessive generation of reactive oxygen species (ROS) through cytochrome P450-2E1 (CYP2E1) mainly in the ER and less in mitochondria [19–25]. CYP2E1, an enzyme responsible for fatty acid omega-oxidation, plays a significant role in promoting oxidative/nitrosative stress, inflammation, and insulin resistance and has been identified as a critical factor in the development of MASH. Increased levels of CYP2E1 have been observed in patients with steatosis and MASH, particularly in the centrilobular region, which corresponds to the site of maximum hepatocellular injury in MASH. CYP2E1 levels are also elevated in obesity, steatosis, and MASH in both humans and rodents. Animal studies have shown that feeding mice with an AIN-76A western diet significantly induces CYP2E1 expression, leading to the development of MASH and fibrosis. Conversely, CYP2E1-null mice are protected from these detrimental effects [21]. Furthermore, CYP2E1 may contribute to excessive lipid accumulation and worsen oxidative stress, thereby inducing hepatic inflammation and causing various forms of hepatocyte damage and death [26]. Hence, targeting CYP2E1 expression is a potentially effective treatment strategy against MASLD and MASH.

The primary objective of the present study is to assess the effectiveness of SNP-630, a novel synthetic molecule, and its metabolites in treating MASH in both animal models and patients with MASH.

Ho *et al. Journal of Translational Medicine*   (2024) 22:936

Page 3 of 18

Methods

In vitro metabolism of SNP-630

SNP-630 was added to human blood containing antibacterial agents methylparaben and propylparaben and incubated at 37 ℃. Samples were collected at the indicated time points, mixed with cold acetonitrile, and centrifuged at 4 ℃ and 13,000 rpm for 5 min. The supernatant was transferred to a tube and stored at −78 ℃ until analysis with HPLC–MS/MS.

An LC–MS/MS assay for the determination of SNP-630 and its four metabolites in human plasma was conducted. Briefly, human plasma samples were spiked with internal standard, processed with solid-phase extraction, and analyzed using reversed-phase HPLC with electrospray ionization, Turbo Ion Spray® MS/MS detection. Negative $(M-H)^-$ ions for SNP-630 and Chlorzoxazone-d3 (Internal standard, IS) were monitored in MRM mode. Analyte-to-IS peak area ratios for the standards were used to create a linear calibration curve using $1/x^2$ weighted least-squares regression analysis.

For metabolite 2 (m2) and metabolite 4 (m4) analysis, human plasma samples were spiked with internal standard, processed by solid-phase extraction, and analyzed using reversed-phase HPLC with electrospray ionization, Turbo Ion Spray® MS/MS detection. Negative $(M-H)^-$ ions for m2, m4, m2-d6 (IS), and Chlorzoxazone-d3 (IS) were monitored in MRM mode. Analyte-to-IS peak area ratios for the standards were used to create a linear calibration curve using $1/x^2$ weighted least-squares regression analysis. For m1 and m3 analysis, human plasma samples were spiked with internal standard, processed via acetylation derivatization, and analyzed using reversed-phase HPLC with electrospray ionization, Turbo Ion Spray® MS/MS detection. Positive $(M+H)^+$ ions for m1, m3, and m1-^{13}C6 (IS) were monitored in MRM mode. Analyte-to-IS peak area ratios for the standards were used to create a linear calibration curve using $1/x^2$ weighted least-squares regression analysis.

In vivo CYP2E1 activity

In vivo, CYP2E1 activity has been previously described [27]. Briefly, high-fat diet (HFD)-fed mice treated with SNP-630 for 12 weeks were fasted overnight and administered an oral dose of chlorzoxazone (8.33 mg/kg) as a probe. Whole blood was then collected via the tail vein 15 min post-administration and stored at −20 ℃ until analysis. Blood concentrations of chlorzoxazone and 6-hydroxychlorzoxazone were measured using LC/MS/MS as described previously [27]. The activity was described as the blood concentration ratios of 6-hydroxychlorzoxazone to chlorzoxazone.

Experimental animal model

Mice were housed in a pathogen-free environment with a 12 h-light/12 h-dark cycle and free access to food and water. All animal husbandry, care, euthanasia, and use procedures followed the guidelines established by the Institutional Animal Care and Use Committees of the National Defense Medical Center (approval number: IACUC-15-309). MASH was induced in male C57BL/6 (B6) mice. The mice were purchased from the National Laboratory Animal Center (Taipei, Taiwan) at the age of 8–10 weeks and housed at the Laboratory Animal Center of the National Defense Medical Center. The mice were fed with a standard diet of 3–5 g/day, provided water ad libitum for 1–2 weeks, and verified to be healthy before initiation of the study. The weight of the mice was recorded once per week.

SNP-630 treatment

B6 mice were allocated randomly to the blank group, vehicle control high-fat diet (HFD) group, and SNP-630 treatment via oral gavage group. Mice in the blank group (n = 8) were fed with a standard diet (13% calories from fat; Laboratory Autoclavable Rodent Diet 5010, LabDiet, Fort Worth, USA); Mice in the HFD group (n = 8) were fed with HFD (60% calories from fat; Research DIETS D12492) for entire study of 30 weeks. Mice in the SNP-630 treatment groups (n = 8/group) were fed with HFD for the entire study duration (30 weeks) and administered 250, 150, 75, or 25 mg/kg SNP-630 once daily by oral gavage for the last 10 weeks of the experiment.

SNP-630-MS treatment

Male B6 mice were used for the SNP-630-MS treatment efficacy tests. MASH was induced with HFD for 21 weeks. The mice were allocated randomly to the blank group, vehicle control HFD group, and SNP-630-MS treatment via oral gavage group. Mice in the blank group (n = 8) were fed a standard diet; mice in the HFD group (n = 8) were fed with HFD (60% calories from fat; Research DIETS D12492) for 21 weeks; mice in the SNP-630-MS treatment groups (n = 8/group) were also fed with HFD and co-administered 62.5/62.5 or 187.5/187.5 mg/kg SNP-630-MS daily for 21 weeks.

Plasma biochemistry of MASH mice

In the animal models, submandibular blood was collected for biochemical tests. At the end of the study, all mice were weighed and euthanized using CO_2. The blood specimens were allowed to clot at 24 ℃ for 1 h, and the serum was separated via centrifugation in a refrigerated centrifuge at $15,700 \times g$ and 4 ℃ for 5 min.

Ho *et al. Journal of Translational Medicine*   (2024) 22:936

Page 4 of 18

Serum ALT levels were subsequently assayed by the National Laboratory Animal Center.

Liver triglyceride (TG) and total cholesterol (TCHO) assays

Animal liver samples were homogenized in 2 mL Folch reagent on ice, centrifuged at $1,977 \times g$ for 20 min at 4 °C, and 1.6 mL of the supernatant was then transferred into a new tube containing 0.8 mL saline. The pellet at the bottom of the centrifuged tube was resuspended in 2 mL of Folch reagent and the mixture was shaken for 20 min, followed by centrifugation at $1,977 \times g$ for 20 min at 4 °C, and 1.6 mL of the supernatant was then transferred to the tube that contained the supernatant from the first-run centrifugation, shaken for 30 s, and centrifuged at $1,977 \times g$ for 20 min at 4 °C. A total of 2 mL of the bottom layer liquid was transferred to a glass container, air dried under a nitrogen stream, and the sample was fully dissolved in EtOH: Triton X-100 (3:1 v:v) with sonication. Liver TG and TCHO levels were analyzed using RANDOX TG and RANDOX CHOL kits, respectively, according to the manufacturer's instructions. Absorbance measurements were performed using an Epoch 2 Microplate Spectrophotometer (BioTek). Liver TG and TCHO levels were calculated using standard curves and normalized to the weight of the liver in the sample.

Histopathological tissue sectioning, staining, and evaluation

Following euthanasia, approximately 1 cm^3 of the largest right lobe of the liver was excised from the same position to eliminate bias due to subjective observation, fixed in 10% neutral formalin, and dehydrated in increasing concentrations of ethanol (30%, 50%, 70%, 95%, and 99.5%), followed by xylene. The fixed tissues were embedded in paraffin and cut into 5-μm sections using a microtome, mounted on clean slides, and dried at 37 °C. To identify lesions, fat accumulation, necrosis, and fibrosis in liver cells due to ongoing liver damage, the liver sections were stained with hematoxylin and eosin (H&E) to evaluate the degree of liver fat accumulation and with Sirius Red to evaluate the degree of fibrosis. Semi-quantitative pathological assessment was performed by a physician or veterinary pathologist in a double-blinded manner to score (NAFLD Activity Score [NAS]). Finally, a differential analysis of the scores for each group was conducted using the Kruskal–Wallis test.

Western blotting

Fifty microgram liver tissues were lysed in RIPA buffer to obtain total proteins, (Cell Signaling Technology, Cat no. 9806) supplemented with protease inhibitors (Roche, Cat no. 5892970001) and phosphatase inhibitors (Roche, Cat no. 4906837001). The samples were incubated for 30 min on ice. Protein concentrations were determined using a BCA Protein Assay Kit (Thermo Fisher Scientific, 23,225). Equal amounts of protein (15 μg) were separated using 10% SDS-PAGE and transferred to a polyvinylidene difluoride membrane (Merck Millipore, IPVH00010). The membranes were blocked with 5% bovine serum albumin (BSA; Sigma-Aldrich, A2058) for 1 h at room temperature and the membranes were incubated with primary antibodies overnight at 4 °C. The utilized primary antibodies were rabbit anti-CYP2E1 (1:1000, Abcam ab28146) and mouse anti-ACTB (1:5000, actin-beta, Abcam ab8226) and secondary antibodies were goat anti-mouse conjugated with HRP (1:10,000, Abcam ab97023), and HRP Donkey anti-rabbit IgG (1:10000, BioLegend Cat no. 406401). The bands were imaged and analyzed with the Image J software (National Institutes of Health, https://imagej.nih.gov/ij/). The relative density was calculated as the ratio of the intensity of the protein of interest to that of ACTB, and all band detection was within the linear range.

Real-time PCR

Total RNA was extracted from 50 mg of mice liver tissue using EasyPure total RNA extraction kit (Bioman Cat no. RT050, Taiwan) and submitted to DNase I treatment (Bioman, Taiwan) according to the manufacturer's protocol. RNA concentration and purity were evaluated using spectrophotometry (Nanodrop One, Thermo Scientific). RNA (1 μg) was reverse-transcribed using iScript cDNA synthesis kit (Bio-rad Cat no. 1708890, USA) in a 20 μL reaction according to manufacturer's protocol. 50 ng of cDNA templates was amplified in duplicates using iTaq universal SYBR green supermix (Bio-rad Cat no. 1725124, USA) on a CFX96 Real-Time PCR System (Bio-rad, USA). Transcripts were amplified using the following program: 5 min at 95 °C followed by 40 cycles of 10 s at 95 °C and 30 s at 60 °C. Relative mRNA expression was quantified using the $2^{-\triangle\triangle\mathrm{Ct}}$ method and *Gapdh* as the housekeeping gene. The following primers were used for Real-Time PCR (5′-3′): Gapdh-Forward: CGTGTTCCTACCCCC AATGT, Gapdh-Reverse: GTTGCTGTTGAAGTC GCAGG, Col1a1-Forward: TTCACCTACAGCACC CTTGT, Col1a1-Reverse:TTGGGGGTGGAGGGAG TTTAC, Col3a1-Forward: CGGCTGAGTTTTATG ACGGG, Col3a1-Reverse: ATAGGACTGACCAAG GTGGC, Timp1-Forward: TGGCATCTGGCATCC TCTTG, Timp1-Reverse: GGTCTCGTTGATTTCTGG GGA, Acta2-Forward: CCCTGGAGAAGAGCTACG

Ho *et al. Journal of Translational Medicine*   (2024) 22:936

Page 5 of 18

AAC, Acta2-Reverse: GACAGGACGTTGTTAGCA TAGAG.

SNP-630-MS clinical study

Study design and patients

We conducted a phase 2 study, comprising a 12-week dosing phase and a 2-week safety follow-up period, in patients with MASH. The individuals enrolled in this study satisfied the following inclusion criteria: (1) age ≥ 20-years-old, body weight ≥ 54 kg, and liver fat content ≥ 10.0% as measured using MRI; (2) phenotypic diagnosis of MASH based on one or more of the following criteria: alanine aminotransferase ALT levels ≥ 1.5 × upper limit of normal (ULN), or ALT ≥ ULN and body mass index (BMI) ≥ 25 and diagnosis of type 2 diabetes mellitus; (3) adequate organ function: hemoglobin ≥ 9 g/dL, platelet count ≥ 100 × 10⁹/L, white blood cell count ≥ 3.0 × 10⁹/L, creatinine clearance ≥ 90 mL/min (determined by the Cockcroft-Gault equation), and serum uric acid < 9.0 mg/dL; and (4) able to provide written informed consent and understand and comply with the requirements of the study.

Individuals were excluded from the study if they met the following exclusion criteria: (1) decompensated or severe liver disease, a history or presence of alcohol abuse, and/or being unable to undergo an MRI scan; (2) having electronically, magnetically, and mechanically activated implanted devices; (3) a significant systemic or major illness other than liver disease; (4) a documented history of a serious allergic reaction to SNP-630-MS or any structurally related compounds; (5) patients with diabetes who did not maintain a stable dose of oral medication for hyperglycemia or had changed their insulin dose by > 10% over the past two months; (6) regularly using agents that are potent against hepatitis or affect lipid metabolism; (7) women who were pregnant or lactating; and (8) women of child-bearing potential who were not committed to taking reliable contraception during their participation in the study and for at least 4 weeks after the end of the study treatment period.

The investigational products (IPs), including study agents and control products, were supplied by the Investigational New Drug (IND) sponsor and shipped to the hospital pharmacy before initiating participant enrollment. We provided the physician investigator with the packaged study agent labeled in accordance with country-specific regulatory requirements. Each open-label period kit contained a supply of IPs sufficient for 5 weeks and 1 week in reserve. The participants were instructed to take a dose, either 800 or 400 mg of SNP-630-MS or the matched placebo once daily after a meal.

The safety profile of the study agent was assessed by monitoring and recording the incidence of treatment-emergent adverse events (TEAEs) and serious TEAEs, whether related to the study treatment or not, as determined by changes in clinical laboratory tests (i.e., hematological and biochemical tests, including iron panels), physical examinations, vital signs, standard electrocardiograms, and any other untoward medical events during the study period. Safety was evaluated for all participants who received at least one dose of study medication.

Primary and secondary endpoints

The primary outcome was the change in serum ALT (also called GPT) at week 12 compared with baseline. This endpoint was based on the US-FDA guidance Noncirrhotic Nonalcoholic Steatohepatitis with Liver Fibrosis: Developing Drugs for Treatment as non-invasive, disease specific biomarker for early phase 2 trials. Secondary outcomes were as follows: (1) percentage changes in ALT, serum aspartate aminotransferase (AST, also called GOT), alkaline phosphatase (Alk-P), gamma-glutamyl transpeptidase (γ-GT), and serum CK-18 fragment levels at week 12 compared with baseline; (2) reduction in liver fat content, measured noninvasively based on the proton density fat fraction (PDFF) on MRI, at completion of week 12 compared with baseline; (3) percentage of patients who experience AE/SAE and those who experience AEs leading to discontinuation at the end of dosing.

Data analysis

Effects of SNP-630 and its metabolites in an animal model of MASH

Data are expressed as means ± standard error (SEM). Statistical significance was determined via one-way analysis of variance using Statistical Package for the Social Sciences, Version 13 (SPSS Inc.). Multiple comparisons were subsequently carried out using post-hoc least significant difference tests to confirm the significance of the differences between groups. Means were considered significantly different at $P < 0.05$. The statistical differences for total NAS were assessed using the Mann–Whitney U-test.

SNP-630-MS clinical study

To investigate the efficacy and safety of SNP-630-MS in patients with MASH, the primary and secondary endpoints at week 12 were compared with the corresponding baseline values. The primary efficacy analysis compared the percentage reduction in ALT, assuming that the participants who received SNP-630-MS would exhibit a significant reduction in liver fat that was superior to baseline at a significance level of 0.05. The absolute values of the primary endpoint and secondary endpoints

Ho *et al. Journal of Translational Medicine*   (2024) 22:936

Page 6 of 18

at week 12 were also compared with the baseline values using paired *t*-tests.

Analysis datasets were planned for the "intention-to-treat (ITT)" population, which was the full analysis set (FAS), including all participants who received at least one dose of the study agent. The per-protocol analysis dataset (PP) was used to define the subset of the participants in the FAS who completed their scheduled visits with no missing ALT values at baseline or week 12. participants in the PP dataset must have taken at least 80% of the investigational product for 80% of the days in the study period, with no major violation of the required procedures of the protocol. The safety population included all participants who received at least one dose of the study agent (ITT).

Subgroup analyses were conducted in several subpopulations, including the "ITT" or "PP" populations by sex, BMI, age, history of alcohol consumption, baseline ALT, baseline liver fat content, and administered dose.

Results

Metabolic pathway and mechanism of action of SNP-630 and SNP-630-MS

When incubated with human whole blood at 37 °C, SNP-630 underwent metabolic processes that led to the formation of four major metabolites (Fig. 1b). The metabolic pathway of SNP-630 is illustrated in Fig. 1a. SNP-630-MS is a mixture of two active metabolites produced by SNP-630 metabolism.
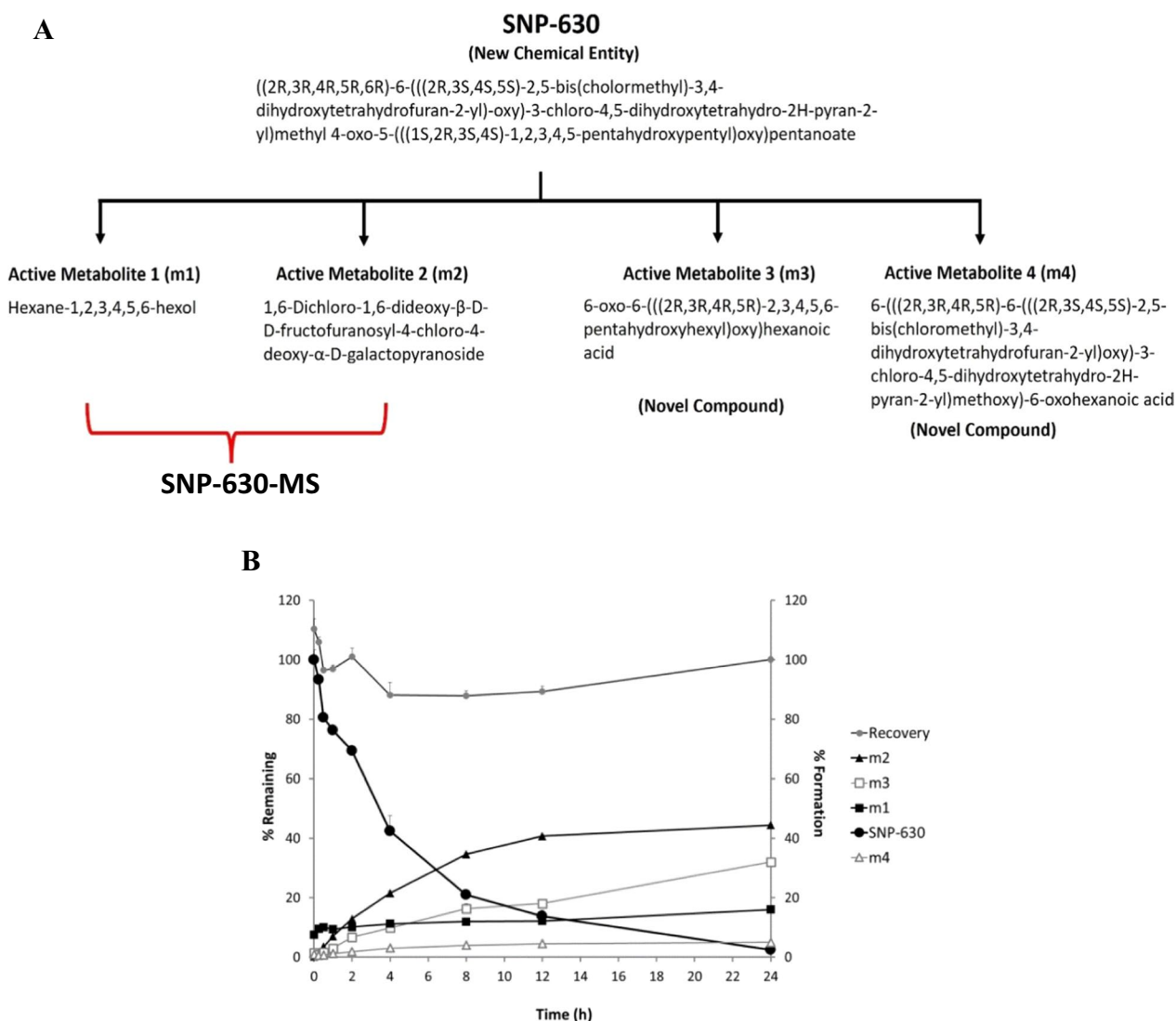

Fig. 1 Metabolic scheme and profile of SNP-630. **a** Schematic illustration of SNP-630 metabolism. The structures of new chemical entities, SNP-630 and SNP-630-MS, are shown. **b** Metabolic profiles of SNP-630 (% remaining) and its metabolites (% formation) in human blood

Ho *et al. Journal of Translational Medicine*   (2024) 22:936

Page 7 of 18

SNP-630 ameliorates HFD-induced hepatic steatosis and inflammation in mice

Considering the induction of CYP2E1 activation and expression in patients with MASLD or MASH [19–25], we were intrigued by the potential of SNP-630 to inhibit CYP2E1 activity and expression in a mouse model of MASLD. We induced MASH in mice with HFD for 20 weeks and administered SNP-630 orally while continuing the HFD for an additional 10 weeks. After 30 weeks of HFD feeding, mice in the HFD group exhibited an increase in CYP2E1 protein expression; however, treatment with SNP-630 significantly inhibited the protein expression and activity of CYP2E1 (Fig. 2a–c), accompanied with a notable decrease in body weight, liver weight/body weight ratio, and hepatic lipid content (triglycerides, TG and cholesterol, T-CHO) (Fig. 2d–f and Additional File 1b). Histological analysis using H&E staining revealed the presence of cytoplasmic fat vacuoles and droplets in the hepatocytes of mice fed with the HFD diet, whereas mice treated with SNP-630 exhibited smaller fatty droplets and reduced ballooning degeneration in hepatocytes (Fig. 2h, i). Furthermore, SNP-630 treatment significantly decreased cytokine and chemokine monocyte chemoattractant protein 1 and CCL4 expression, further indicating the reduction in hepatic inflammation (Additional File 1c, d). The increase in liver injury biomarkers induced by the HFD was restored by SNP-630, as evidenced by remarkably decreased serum ALT activities (Fig. 2g).

To assess the progression of steatohepatitis in mice, we evaluated the extent of liver fibrosis. Mice fed with HFD exhibited a greater area of fibrils stained with Sirius Red, while treatment with SNP-630 resulted in a significant reduction in hepatic fibrosis in these mice (Fig. 2h, j). Additionally, we examined the expression levels of fibrogenic genes, *Co1a1*, *Col3a1*, and *Timp1*. As depicted in Fig. 2, the expression of these fibrogenic genes was upregulated in mice fed with HFD compared with those fed with a normal diet. Notably, treatment with SNP-630 led to a significant reduction in the expression of

these fibrotic genes, further supporting the evidence of reduced liver injury by SNP-630 (Fig. 2j-l and Additional File 1e).

Recently, studies reported the role of LPS from the gut microbiota in favoring the occurrence of MASH. Interestingly, SNP-630 normalized the elevated LPS levels in HFD diet-fed mice (unpublished data).

SNP-630-MS, active metabolites of SNP-630, ameliorates HFD-induced hepatic steatosis and inflammation in mice

Given the rapid conversion of SNP-630 into four active metabolites in vivo, we next determined whether the amelioration of HFD-induced MASH by SNP-630 is mediated through its active metabolites. Two of these active metabolites were synthesized and combined to create SNP-630-MS (Fig. 1a). To assess the hepatoprotective effects of SNP-630-MS in MASH, mice were fed with HFD for 21 weeks. SNP-630-MS significantly reduced the weight gain and protein expression of CYP2E1 (Fig. 3a and Additional File 1a). The levels of liver TG and TCHO were elevated in the HFD group compared with the control group. In contrast, administration of SNP-630-MS resulted in a decrease in liver/body weight ratio, hepatic TG, and TCHO levels in treated mice (Fig. 3b-d). Additionally, the HFD group exhibited elevated ALT levels, whereas mice treated with SNP-630-MS showed significantly reduced ALT levels (Fig. 3e).

Histological analysis using H&E staining uncovered notable steatosis, inflammation, and hepatic ballooning in the livers of mice fed with HFD, leading to an average NAFLD Activity Score (NAS) of 3.7. Conversely, mice treated with a high dose of SNP-630-MS displayed diminished hepatic steatotic vesicles, inflammation, and ballooning, resulting in an average NAS of 1.3 (Fig. 3f). Furthermore, the fibrosis score was significantly increased in HFD-induced mice compared with those on a chow diet, however, administration of SNP-630-MS dose-dependently attenuated the fibrosis levels and the expression of fibrotic genes *Col3a1* and *Timp-1* (Fig. 3g-i). These findings suggest that SNP-630-MS inhibited

(See figure on next page.)

Fig. 2 SNP-630 treatment alleviates HFD-induced hepatic steatosis, inflammation, and fibrosis in the MASH mouse model. **a** SNP-630 inhibits CYP2E1 catalytic activity. The metabolic ratios of chlorzoxazone (CZX) and its CYP2E1-drived metabolite, 6-hydroxychlorzoxazone (6-OH-CZX), in mice are plotted versus the SNP-630 treatment dose. Data are presented as mean ± SE (*n* = 8 for each group). **b** Representative immunoblots of SNP-630 treatment significantly reduced CYP2E1 protein expression. Western blotting of CYP2E1 and β-actin was performed in mouse liver lysates. **c** Quantification of CYP2E1 protein expression level. **d** Liver/body weight ratio **(e)** Liver TG **(f)** Liver total cholesterol. **g** ALT **h** Histopathological analysis of liver tissues. Representative images of Sirius red (left) and H&E (right) staining of livers from the blank group, HFD group, and SNP-630 250 mg/kg group (scale bar: 50 μm). **i** NAFLD Activity Score (NAS) **(j)** Hepatic collagen deposition. Fields from Sirius red-stained sections were scanned using a slide scanner (Axio Scan.Z1), and the fibrotic area was measured with digital image analysis using the ImageJ software **(k)** Representative results of expression of hepatic *Col3a1* mRNA. **l** Representative results of expression of hepatic *Timp1* mRNA. Data are expressed as mean ± SEM. Statistical analyses were carried out using a one-way analysis of variance (n = 8/each group). MASH: Metabolic dysfunction-associated steatohepatitis; HFD: high-fat diet

Ho *et al. Journal of Translational Medicine*   (2024) 22:936

Page 8 of 18
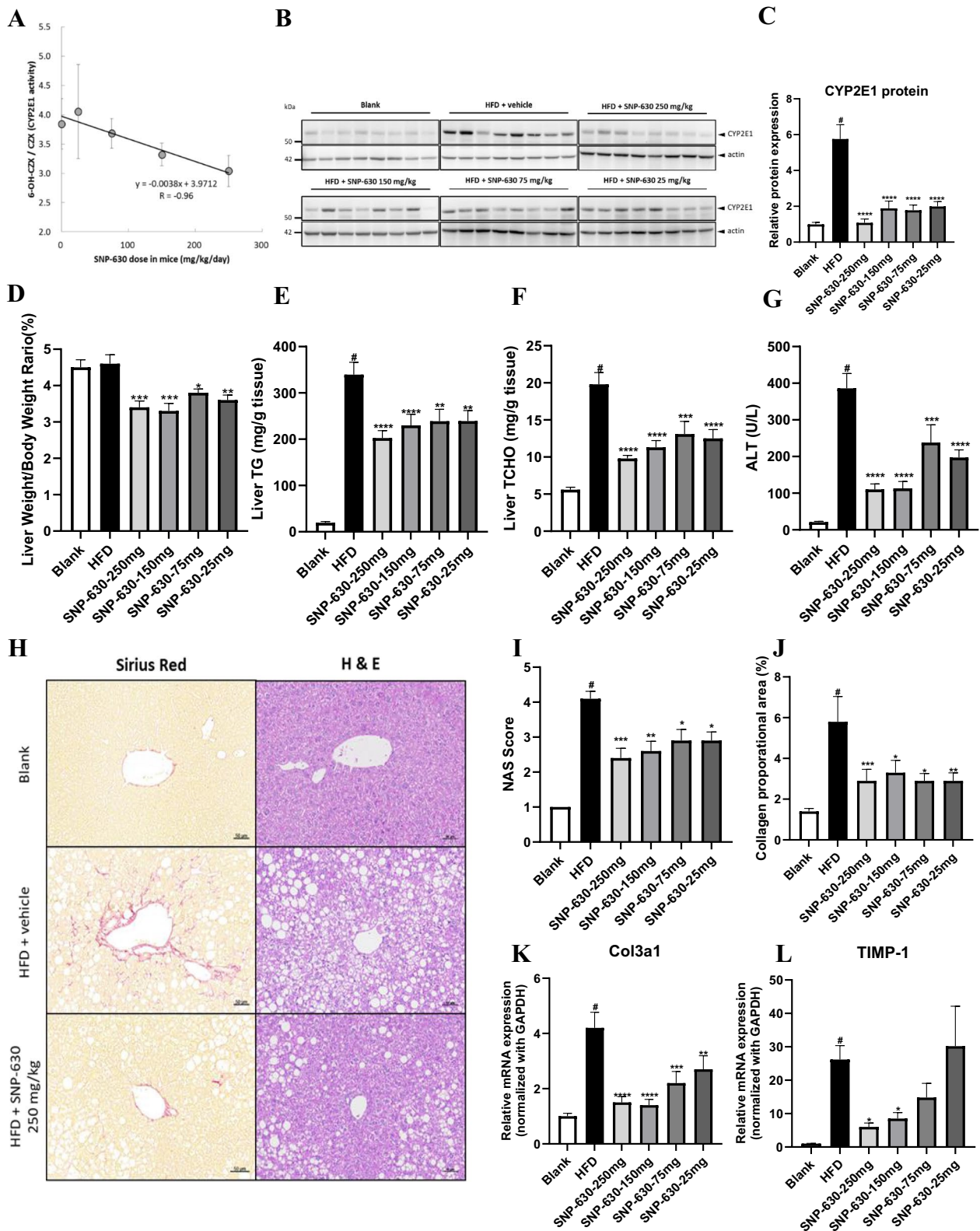
Fig. 2 (See legend on previous page.)

Ho *et al. Journal of Translational Medicine*   (2024) 22:936

Page 9 of 18

Fig. 3 Hepaprotective effects of SNP-630-MS on the HFD-induced mouse model of MASH. MASH was induced in male C57BL/6 mice with HFD for 21 weeks. HFD-induced MASH mice were divided into three groups and received an HFD along with vehicle, 187.5/187.5 (assigned as SNP-630-MS-High), or 62.5/62.5 mg/kg SNP-630-MS (assigned as SNP-630-MS-Low) by oral gavage once daily. Mice on a normal chow diet received the vehicle as the normal control (blank group). **a** Body weight, **b** liver/body weight ratio, **c** liver TG, **d** liver TCHO, **e** ALT, **f** NAS, **g** fibrosis stage, **h** expression of hepatic *Col3a1* mRNA, and **(i)** expression of hepatic *Timp1* mRNA. Data are expressed as mean ± SEM. Statistical analyses were carried out using a one-way analysis of variance (n = 12/each group). MASH: Metabolic dysfunction-associated steatohepatitis; HFD: high-fat diet
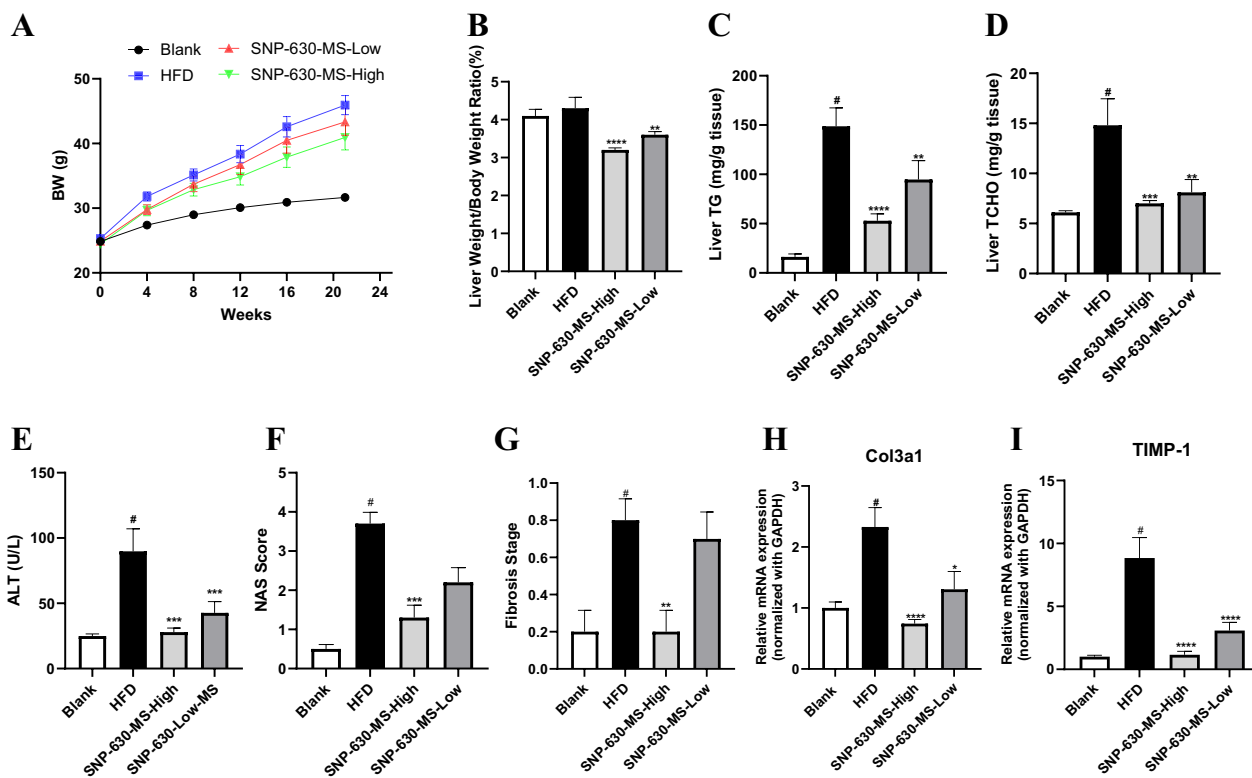
the pathological progression of HFD-induced MASLD by reducing hepatic lipid accumulation, improving NAS, and preventing liver injury.

Long-term application of SNP-630 and SNP-630-MS was safe in mice

The long-term safety of SNP-630 and SNP-630-MS was assessed in mice. No abnormal findings were observed in the liver, kidney, spleen, or heart of mice treated with SNP-630 and SNP-630-MS. Additionally, no diseases or abnormal clinical findings related to the administration of SNP-630 and SNP-630-MS were observed during necropsy studies conducted at the end of the experiment (Data not shown). These findings indicate that both compounds are safe for long-term use.

Clinical trial of SNP-630-MS
Participants and baseline characteristics
This open-label study was initiated at Tri-Service General Hospital, a participating medical center in Taiwan. A total of 90 patients with MASH were screened for

enrollment, of which 17 were enrolled in the first arm, receiving two tablets of SNP-630-MS, assigned as high dose group, and 18 in the second arm, receiving one tablet of SNP-630-MS, assigned as low dose group. One patient (5.9%) in the first arm withdrew voluntarily after 3 days of SNP-630-MS dosing. The schematic of the clinical trial progress is presented in Fig. 4.

The baseline demographics and disease characteristics of the participants were evenly distributed between the two dosing groups, as shown in Table 1. The mean age of the participants was 44.45 years, with 83% being male and a mean body mass index of 30.5 kg/m^2. Approximately 51.42% of the patients had diabetes or pre-diabetes. All patients met the liver enzyme entry criteria for this study.

Primary outcome
In the primary efficacy analysis, conducted on the mITT population, those participants were included who had undergone eligible screening and had at least one post-dosing measurement. Patients treated with SNP-630-MS
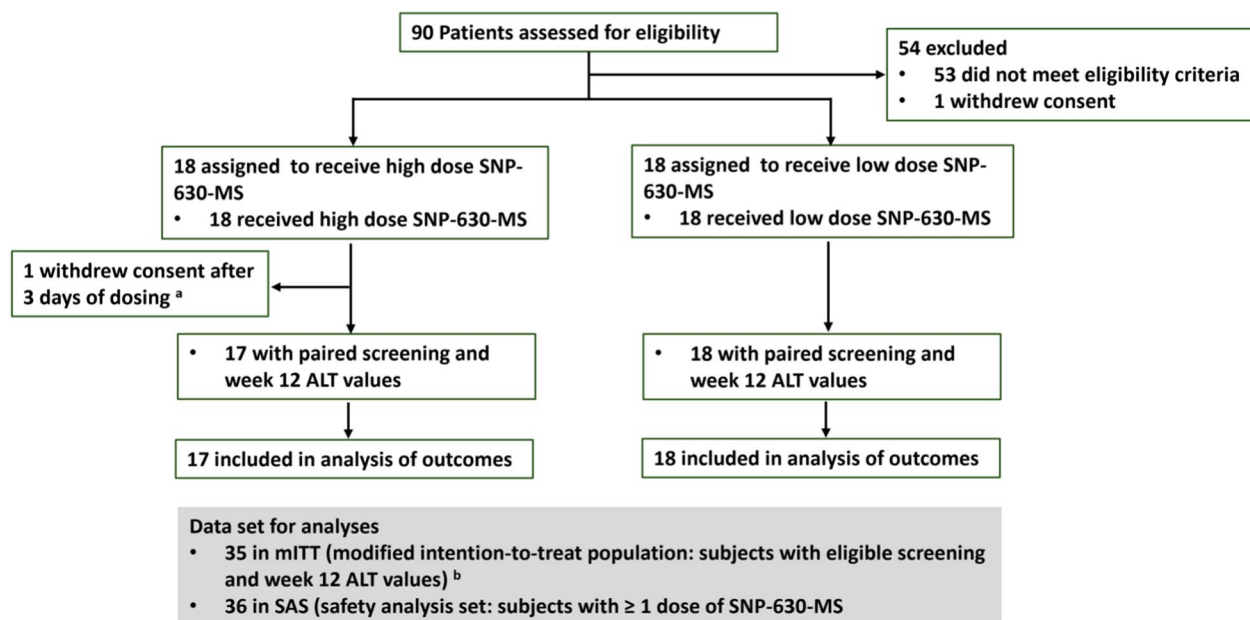
Ho *et al. Journal of Translational Medicine*   (2024) 22:936

Page 10 of 18

Fig. 4 SNP-630-MS clinical trial profile. **a** The disposition of one participant who withdrew after 3 days of dosing cannot be reported. **b** Analysis of primary efficacy for the modified intention-to-treat (mITT) population. ALT: alanine aminotransferase

exhibited a dose-dependent reduction in serum ALT levels at week 12 compared with baseline (-29.5 ± 33.0 U/L, $P = 0.002$ for high-dose SNP-630-MS and -18.9 ± 27.3 U/L, $P = 0.009$ for low-dose SNP-630-MS). The decrease in serum ALT was observed during the first 8 weeks of SNP-630-MS dosing and sustained throughout the treatment period (Fig. 5a).

Considering that MASLD is a heterogeneous condition influenced by various factors such as demographics, metabolic status, and genetic predisposition [28], subgroup analyses were conducted to assess the relationship between ALT reduction and these factors (Fig. 5b). After adjusting for all potential confounding variables, a significant association was observed between ALT reduction and SNP-630-MS treatment in all analyzed subgroups, including age group, sex, obesity status, *PNPLA3* genotype, fibrosis stage, and diabetes.

Key secondary and exploratory outcomes
Significant reductions in serum AST (-13.1 ± 23.2 U/L, $P = 0.034$) and lactate dehydrogenase (LDH, -20.2 ± 38.0 U/L, $P = 0.044$) were observed after 12 weeks of treatment with two tablets of SNP-630-MS (Table 2). Notably, SNP-630-MS treatment significantly improved glycemic control. Fasting serum glucose levels showed a significant reduction (-19.9 ± 30.3 U/L, $P = 0.016$; Table 2), and there was a slight decrease in insulin levels and HOMA-IR, indicating lower insulin resistance after administration of two tablets of SNP-630-MS at week 12 compared

with baseline. Furthermore, SNP-630-MS treatment was associated with significant reductions in both relative and absolute hepatic fat fraction compared with baseline (Table 2). Favorable decreases were also observed in plasma lipid and lipoprotein levels.

Total cholesterol levels decreased by an average of 18.4 mg/dL and triglyceride levels decreased by 37.8 mg/dL in the high-dose group. Finally, participants receiving the higher dose experienced an average reduction of 0.5 kg/m^2 in BMI (Table 2).

Significant reductions were also observed in the circulating levels of cytokines and chemokines involved in liver inflammation and fibrosis, such as CCL4, CCL5, and caspase 3, after 12 weeks of SNP-630-MS dosing (Table 2). Furthermore, liver stiffness, as measured using FibroScan, showed a significant decrease ($P = 0.03$) in patients with F4 stage fibrosis who received SNP-630-MS treatment (Fig. 5c). These findings indicate the potential of SNP-630-MS to reduce liver inflammation and fibrosis in patients with MASH.

Safety and tolerability
The safety analysis included all 36 patients with MASH who received at least one dose of the study agent. Adverse events were generally mild and unrelated to the treatment. Throughout the study, a total of four treatment-unrelated adverse events were reported, including acute bronchitis, acute pharyngitis, acute sinusitis, and arthropathy. These adverse events were determined to be

Ho *et al. Journal of Translational Medicine*   (2024) 22:936

Page 11 of 18

Table 1 Demographic and clinical characteristics at baseline

Characteristic, mean (SD)	SNP-630-MS HD QD n = 17		SNP-630-MS LD QD n = 18	
Demographics				
Age, years	46.1	(10.9)	42.9	(12.9)
Female sex, n (%)	4	(23.5%)	2	(11.1%)
Liver enzymes				
ALT, U/L	115.1	(29.7)	111.6	(23.8)
AST, U/L	65.4	(31.5)	58.2	(17.4)
Gamma-glutamyl transferase, U/L	72.4	(27.5)	61.8	(38.5)
Alkaline phosphatase, U/L	66.3	(16.3)	56.4	(13.3)
Total bilirubin, mg/dL	0.6	(0.1)	0.7	(0.3)
Lactic dehydrogenase, U/L	219.8	(48.3)	181.9	(34.7)
Lipids				
Total cholesterol, mg/dL	197.8	(34.6)	185.8	(37.0)
HDL cholesterol, mg/dL	43.9	(6.4)	42.8	(9.6)
LDL cholesterol, mg/dL	125.4	(29.9)	118.2	(29.3)
LDL/HDL	2.9	(0.6)	2.9	(0.9)
Triglycerides, mg/dL	225.1	(91.7)	191.0	(109.1)
Metabolic factors				
Fasting serum glucose, mg/dL	117.9	(36.3)	109.9	(26.0)
Insulin, mIU/L	28.6	(30.7)	19.2	(10.5)
HOMA-IR, glucose [mg/dL] × insulin [mIU/L]/405	9.7	(12.5)	5.5	(4.5)
Glycated hemoglobin A1c, %	6.1	(0.8)	6.4	(1.0)
Weight, kg	84.2	(10.9)	89.5	(14.1)
Body mass index, kg/m^2	30.4	(2.7)	30.6	(4.4)
Waist circumference, cm	96.2	(9.1)	100.5	(9.1)
Systolic blood pressure, mm Hg	132.2	(12.2)	131.4	(14.7)
Diastolic blood pressure, mm Hg	79.6	(6.9)	79.2	(7.7)
Imaging				
MRI-PDFF, %	14.8	(5.4)	21.2	(7.2)
FibroScan, kPa	10.9	(7.0)	9.0	(5.2)
Chemistries				
Creatinine, mg/dL	0.9	(0.2)	0.9	(0.1)
Blood urine nitrogen, mg/dL	14.2	(3.9)	14.1	(3.2)
Calcium, mg/dL	9.7	(0.3)	9.6	(0.4)
Phosphate, mg/dL	3.4	(0.5)	3.7	(0.4)
Sodium, mmol/L	139.3	(2.1)	139.8	(1.9)
Potassium, mmol/L	4.0	(0.3)	4.0	(0.3)
Chloride, mmol/L	102.8	(2.4)	103.7	(2.3)
Uric acid, mg/dL	6.9	(1.4)	6.8	(1.5)
Albumin, g/dL	4.7	(0.3)	4.6	(0.3)
Total protein, g/dL	7.4	(0.5)	7.3	(0.4)

Data are expressed as *n* (%) or mean (SD). *ALT* alanine aminotransferase, *AST* aspartate aminotransferase, *HDL* high-density lipoprotein, *LDL* low-density lipoprotein, *HOMA-IR* homoeostasis model assessment–estimated insulin resistance, *SD* standard deviation

of "mild" intensity by the investigators. Importantly, no serious adverse events were reported in this trial as of the writing of this manuscript, indicating the favorable safety profile of the treatment.

Discussion

Despite significant progress in understanding the pathogenesis of MASLD and efforts to develop therapeutic interventions, there remain substantial challenges and no approved treatment for this disease. In recent years, pharmaceutical companies have unsuccessfully attempted to develop effective drugs for MASH, primarily due to a lack of efficacy, toxicity concerns, or a combination of both [29].

Most clinical trials for MASH have traditionally focused on single-agent (monotherapy) approaches. However, considering the complex pathophysiology of the disease and the presence of multiple escape pathways, it is increasingly evident that developing a single drug capable of effectively treating most patients is becoming more challenging and less likely to succeed [30]. As a result, there is growing recognition among drug developers that a single agent or a combination of therapies with different but complementary mechanisms of action may offer the best approach to enhance efficacy, slow disease progression, or even reverse MASH [31]. This shift toward combination therapies is aimed at targeting multiple pathways and achieving synergistic effects to address the heterogeneity of MASH and improve treatment outcomes.

In this study, we conducted a comprehensive investigation to evaluate the therapeutic potential of SNP-630 and its metabolites (SNP-630-MS) with multiple mechanisms in the context of MASH. Initially, we demonstrated that both SNP-630 and SNP-630-MS could effectively inhibit the activity of CYP2E1 enzyme in vivo (Fig. 2a), and expression of CYP2E1 enzyme in animal models of MASH (Fig. 2 b, c and Additional File 1a), subsequently reducing hepatic lipid accumulation, inflammation, and fibrogenesis (Fig. 2). These findings highlight the multifaceted therapeutic effects of SNP-630 and its metabolites, making them promising candidates for the treatment of MASH. Building upon this evidence, we proceeded to administer SNP-630-MS to patients with MASH to confirm the efficacy and safety observed in preclinical studies, further validating the potential of SNP-630 as a therapeutic intervention for MASH.
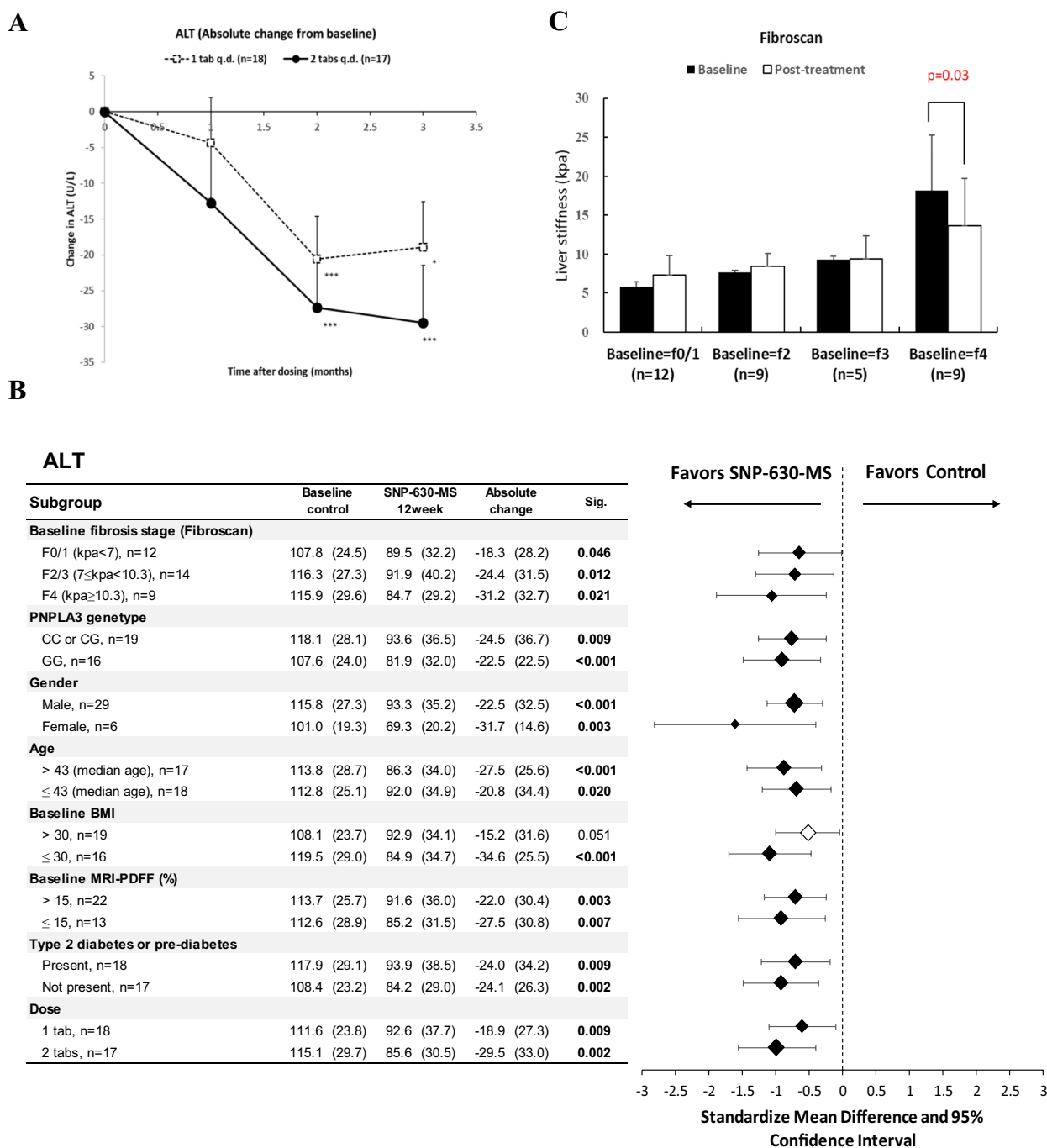
Ho et al. Journal of Translational Medicine   (2024) 22:936

Page 12 of 18

A

B

ALT

Subgroup	Baseline control	SNP-630-MS 12week	Absolute change	Sig.
Baseline fibrosis stage (Fibroscan)				
F0/1 (kpa<7), n=12	107.8 (24.5)	89.5 (32.2)	-18.3 (28.2)	**0.046**
F2/3 (7≤kpa<10.3), n=14	116.3 (27.3)	91.9 (40.2)	-24.4 (31.5)	**0.012**
F4 (kpa≥10.3), n=9	115.9 (29.6)	84.7 (29.2)	-31.2 (32.7)	**0.021**
PNPLA3 genetype				
CC or CG, n=19	118.1 (28.1)	93.6 (36.5)	-24.5 (36.7)	**0.009**
GG, n=16	107.6 (24.0)	81.9 (32.0)	-22.5 (22.5)	**<0.001**
Gender				
Male, n=29	115.8 (27.3)	93.3 (35.2)	-22.5 (32.5)	**<0.001**
Female, n=6	101.0 (19.3)	69.3 (20.2)	-31.7 (14.6)	**0.003**
Age				
> 43 (median age), n=17	113.8 (28.7)	86.3 (34.0)	-27.5 (25.6)	**<0.001**
≤ 43 (median age), n=18	112.8 (25.1)	92.0 (34.9)	-20.8 (34.4)	**0.020**
Baseline BMI				
> 30, n=19	108.1 (23.7)	92.9 (34.1)	-15.2 (31.6)	0.051
≤ 30, n=16	119.5 (29.0)	84.9 (34.7)	-34.6 (25.5)	**<0.001**
Baseline MRI-PDFF (%)				
> 15, n=22	113.7 (25.7)	91.6 (36.0)	-22.0 (30.4)	**0.003**
≤ 15, n=13	112.6 (28.9)	85.2 (31.5)	-27.5 (30.8)	**0.007**
Type 2 diabetes or pre-diabetes				
Present, n=18	117.9 (29.1)	93.9 (38.5)	-24.0 (34.2)	**0.009**
Not present, n=17	108.4 (23.2)	84.2 (29.0)	-24.1 (26.3)	**0.002**
Dose				
1 tab, n=18	111.6 (23.8)	92.6 (37.7)	-18.9 (27.3)	**0.009**
2 tabs, n=17	115.1 (29.7)	85.6 (30.5)	-29.5 (33.0)	**0.002**

C

Fig. 5 SNP-630-MS met the primary endpoint of improvement in ALT after 12-week treatment in mITT population. **a** Participants meet the primary endpoint (improvement in ALT). Mean changes from baseline during treatment with two SNP-630-MS tablets (n = 17) and one SNP-630-MS tablet (n = 18) daily for up to 12 weeks. Error bars show standard errors. *P < 0·05, ***P < 0.005 compared with baseline. **b** Comparison of the FibroScan results at different stages. Mean ± standard deviation (n = 5–12). **c** Subgroup analyses for the primary endpoint of reduction in ALT levels. Response by baseline fibrosis stage (FibroScan), PNPLA3 genotype, sex, age, BMI, MRI-PDFF, type 2 diabetes, and dose. *mITT* modified intention-to-treat, *PNPLA3* patatin-like phospholipase domain-containing protein 3, *BMI* body mass index, *MRI-PDFF* magnetic resonance imaging-proton density fat fraction, *ALT* alanine aminotransferase

Table 2 Demographic and clinical characteristics at baseline and week 12 following SNP-630-MS treatment

Characteristic, mean (SD)	SNP-630-MS 400/400 mg 2 tabs QD (n = 17)					SNP-630-MS 400/400 mg 1 tab QD (n = 18)				
	Absolute change from baseline		Percent change from baseline			Absolute change from baseline		Percent change from baseline		
Liver enzymes										
ALT, U/L	−29.5	(33.0)	−23.8	(24.4)	***	−18.9	(27.3)	−17.9	(26.5)	**
AST, U/L	−13.1	(23.2)	−16.6	(29.4)	*	−6.9	(24.0)	−7.2	(36.7)	
Gamma-glutamyl transferase, U/L	−5.4	(16.8)	−6.5	(23.2)		−9.3	(19.8)	−7.2	(32.6)	
Alkaline phosphatase, U/L	−2.9	(8.8)	−3.5	(11.8)		1.1	(6.2)	1.2	(10.4)	
Total bilirubin, mg/dL	0.1	(0.2)	30.2	(45.8)		0.0	(0.2)	4.7	(28.7)	
Lactic dehydrogenase, U/L	−20.2	(38.0)	−7.3	(14.8)	*	8.7	(74.2)	7.5	(42.3)	
Lipids										
Total cholesterol, mg/dL	18.4	(23.8)	9.7	(12.6)		4.6	(19.1)	3.1	(11.1)	
HDL cholesterol, mg/dL	1.5	(5.6)	4.8	(15.5)		7.3	(15.1)	7.3	(13.5)	
LDL cholesterol, mg/dL	8.8	(21.3)	8.5	(18.8)		0.7	(6.7)	2.7	(17.6)	
LDL/HDL	0.1	(0.4)	4.1	(16.2)		0.1	(0.4)	6.0	(15.3)	
Triglycerides, mg/dL	37.8	(213.3)	21.3	(85.9)		1.2	(89.5)	4.5	(55.2)	
Metabolic factors										
Fasting serum glucose, mg/dL	−19.9	(30.3)	−12.4	(19.0)	*	−12.0	(15.9)	−9.8	(12.1)	**
Insulin, mIU/L	−12.8	(31.8)	−8.0	(54.0)		−0.3	(11.6)	2.2	(49.5)	
HOMA-IR, glucose [mg/dL] × insulin [mIU/L]/405	−5.8	(12.8)	−12.2	(62.7)		−0.7	(2.9)	−9.3	(43.3)	
Glycated hemoglobin A1c, %	0.0	(0.2)	-0.1	(3.3)		0.0	(0.5)	-0.4	(6.6)	
Weight, kg	−1.3	(1.6)	−1.7	(2.0)		−1.1	(2.2)	−1.4	(2.7)	
Body mass index, kg/m²	−0.5	(0.6)	−1.7	(2.0)	**	−0.4	(0.8)	−1.4	(2.7)	*
Waist circumference, cm	−0.2	(1.5)	0.2	(1.5)	***	−0.3	(1.5)	−0.3	(1.5)	*
Systolic blood pressure, mm Hg	6.3	(8.8)	4.9	(6.7)		−2.4	(5.4)	−1.8	(4.3)	
Diastolic blood pressure, mm Hg	6.6	(9.0)	8.6	(10.8)		−0.1	(4.1)	0.1	(5.2)	
Imaging										
MRI-PDFF, %	0.1	(4.3)	−3.0	(26.4)		−2.5	(4.4)	−14.5	(21.8)	*
FibroScan, kPa	−0.7	(4.7)	6.5	(42.3)		−0.2	(2.9)	4.8	(37.3)	
Other laboratory results§										
Casepase-3, ng/mL †	−4.2	(6.5)	−15.4	(119.5)	*	−3.3	(10.4)	0.0	(0.9)	
TIMP-1, ng/mL #	−95.7	(200.1)	0.4	(87.4)		−82.3	(175.4)	−0.2	(0.3)	
CCL2, pg/mL #	−17.2	(44.8)	7.0	(94.1)		−0.6	(26.9)	0.2	(0.7)	
CCL4, pg/mL #	−21.2	(30.4)	−35.8	(44.3)	*	−40.2	(100.5)	0.2	(1.1)	
CCL5, ng/mL $	−10.4	(17.2)	−27.5	(87.3)	*	−4.8	(9.0)	0.0	(1.2)	
IL-1 beta, pg/mL †	−3.1	(5.2)	−19.0	(43.2)		−2.6	(11.1)	0.0	(0.6)	

Data are expressed as *n* (%) or means (standard deviation)

ALT alanine aminotransferase, *AST* aspartate aminotransferase, *HDL* high-density lipoprotein, *LDL* low-density lipoprotein, *HOMA-IR* homoeostasis model assessment–estimated insulin resistance, *CCL2* chemokine (C–C motif) ligand 2, also referred to as monocyte chemoattractant protein 1; *CCL4* chemokine (C–C motif) ligand 4, also known as macrophage inflammatory protein-1β; chemokine (C–C motif) ligand 5, also known as regulated on activation, normal T cell expressed and secreted (RANTES); IL-1 beta, interleukin 1 beta; SD: standard deviation. *$P < 0.05$, **$P < 0.01$, ***$P < 0.005$ compared to baseline

§ In other laboratory results, *n* = 16 for the two tablets. For the one-tablet results

† *n* = 4

n = 7

$ *n* = 6

SNP-630 and its active metabolites possess multiple potential mechanisms of action, specifically targeting the underlying pathogenic pathways implicated in MASH. Studies have elucidated that hepatic DNL, characterized by an abnormal increase in newly synthesized fatty acids in the liver, plays a pivotal role in the development of steatosis and the progression of MASLD [32, 33]. Key regulators involved in this process include SREBP-1c, which

Ho *et al. Journal of Translational Medicine*   (2024) 22:936

Page 14 of 18

controls the transcription of genes related to hepatic triglyceride synthesis, and PPARα, responsible for regulating gene transcription involved in fatty acid esterification and oxidation [34, 35]. Additionally, evidence suggests that CYP2E1, by inhibiting PPARα and enhancing SREBP-1c, can impact fat synthesis and metabolism [36, 37]. Therefore, SNP-630 and its metabolites effectively target these regulatory factors, exerting a modulatory effect on hepatic de novo lipogenesis and associated metabolic pathways. By intervening at these crucial points, SNP-630 and its metabolites demonstrate their potential to mitigate the pathogenesis of MASH and contribute to the management of the disease.

Moreover, the activation of resident hepatic macrophages, known as Kupffer cells, occurs in response to gut-derived LPS, saturated fatty acids, cytokines, and injured hepatocytes and triggers the release of proinflammatory cytokines, such as interleukin-1beta (IL-1β), IL-6, and tumor necrosis factor-alpha (TNF-α), through Toll-like receptor 4 (TLR4) activation [38]. Notably, macrophages exhibiting elevated expression of CYP2E1 show increased levels of CD14 and its co-receptor TLR4, as well as enhanced activation of the transcription factor NF-κB [39]. This increased expression of CYP2E1 primes macrophages, rendering them more responsive to lipopolysaccharide stimuli and leading to heightened production of TNF-α [40, 41]. These findings suggest that SNP-630 and its active metabolites, such as SNP-630-MS, modulate Kupffer cell activation by regulating the activity and expression of CYP2E1. However, further validation is necessary to confirm this hypothesis. Nonetheless, these insights highlight a potential mechanism through which SNP-630 and its metabolites could impact the activation of hepatic macrophages and the subsequent inflammatory response in the context of MASH. Growing investigations held the intestinal barrier dysfunction blame for inflaming the MASLD progression. During the initiation and progression of MASH, large amounts of gut bacterial metabolites and bacterial components such as LPS enter the liver through the portal vein due to the intestinal barrier disruption with the increased intestinal permeability. Mice treated with SNP-630 or SNP-630-MS showed normalized LPS levels compared with HFD control (unpublished data), suggesting that SNP-630 and SNP-630-MS might also improve intestinal function. Further studies are warranted to confirm this speculation.

Furthermore, emerging evidence suggests that adaptive immune mechanisms play crucial roles in the progression of steatosis, insulin resistance, inflammation, and fibrosis in MASH [42, 43]. Experimental models of steatohepatitis and patients with MASH have shown increased recruitment of CD4+ and CD8+ T cells to the liver [44, 45]. The elevated numbers of CD4 and CD8 T cells in the liver are associated with higher frequencies of IFNγ-expressing CD4 and CD8 T cells in the blood of patients with MASH, respectively [45, 46]. Additionally, plasma levels of IFNγ correlate positively with the presence and size of hepatic lymphocyte aggregates, as well as the severity of fibrosis. Recent studies have suggested that one of the active metabolites of SNP-630 exhibits immunomodulatory effects by limiting T cell proliferation and differentiation [47]. This finding suggests that SNP-630 alleviates MASH by inhibiting T-cell infiltration in the liver, although further confirmation is required. Furthermore, another active metabolite of SNP-630 has a dual regulatory role in promoting fat browning and enhancing lipid homeostasis in cultured white adipocytes [48]. Collectively, these studies provide support for the potential anti-MASH properties of SNP-630 and its active metabolites through the regulation of lipid metabolism, Kupffer cell activation, T-cell infiltration, and intestinal function.

In the present phase 2 trial of patients with MASH, SNP-630-MS, an active metabolite of SNP-630, was utilized as a proof-of-concept. This open-label study evaluated the efficacy of SNP-630-MS in treating MASH. After 12 weeks of treatment, significant anti-inflammatory effects were observed, as evidenced by a substantial decrease in serum ALT levels from baseline (Fig. 5a). The reduction in ALT was −18.9 U/L for SNP-630-MS (one tablet) and −29.5 U/L for SNP-630-MS (two tablets). Interestingly, when compared with Ocaliva from Intercept and Resmetirom from Madrigal, both of which have shown improvement in MASH during phase 3 trials, SNP-630-MS exhibited stronger efficacy in reducing ALT levels and demonstrated better safety and tolerability profiles than these other candidate drugs at a similar stage of development [49, 50].

The predisposition to MASLD is influenced by various genetic polymorphisms. Among these genetic variants, the *PNPLA-3* rs738409 C > G (I148C/G-G/G) genotype is considered a common determinant of MASLD [51]. Patients with this genotype are associated with higher liver fat accumulation, increased risk of fibrosis, and reduced benefits from treatments compared with those with the wild-type genotype [52, 53]. In our study, we observed a significant reduction in serum ALT levels after SNP-630-MS treatment specifically in patients with *PNPLA3* rs738409 GG or wild-type genotype (Fig. 5b). MASLD often coexists with type 2 diabetes (T2DM), but the impact of T2DM on the efficacy of the drug remains unclear. Subgroup analysis revealed that SNP-630-MS was effective in both patients with and without T2DM (Fig. 5b). Additionally, fasting glucose and HOMA-IR, markers of glucose metabolism, showed significant improvements in patients treated with SNP-630-MS (Table 2). These findings suggest that SNP-630-MS

Ho *et al. Journal of Translational Medicine*   (2024) 22:936

Page 15 of 18

may have potential pharmacological benefits in treating T2DM, although further research is required to fully comprehend its clinical implications.Consistent with the findings from our animal studies (Figs. 2 and 3), SNP-630-MS demonstrated anti-steatosis activity in patients with MASH. Specifically, the low-dose group showed a significant reduction of 14.5% in MRI-PDFF, indicating a decrease in liver fat content (Table 2). However, in the high-dose group, no significant decrease was observed in MRI-PDFF, possibly due to the presence of outliers in the dataset. To address this, we applied the interquartile rule to identify and remove outliers from the data. After eliminating the outliers, we observed a significant reduction of 10.2% in MRI-PDFF in the high-dose SNP-630-MS group. Nevertheless, it is important to note that further experiments are required to validate these results.

Furthermore, SNP-630-MS exhibited strong anti-fibrotic potential by significantly reducing fibrogenesis-related biomarkers. Liver inflammation, which plays a crucial role in fibrosis development, is regulated by CC chemokines that control important chemokine pathways [54]. Notably, treatment with SNP-630-MS resulted in a significant decrease in serum levels of CCL4 and CCL5 in patients with MASH, indicating its effectiveness in suppressing the fibrogenic response (Table 2). Additionally, FibroScan measurements demonstrated the efficacy of SNP-630-MS in improving liver fibrosis. Interestingly, after 12 weeks of SNP-630-MS treatment, there was a significant reduction in liver stiffness (kPa) among patients with a baseline FibroScan fibrosis score of F4, indicating the potential of SNP-630-MS to ameliorate liver fibrosis (Fig. 5c).

SNP-630-MS was generally well tolerated; no SAE was reported in this study. Data on human exposure to each of the components of SNP-630-MS have been well-established and reported in a comprehensive series of toxicological studies. Therefore, the safety issues had already been evaluated and none were expected.

No more than approximately 40% of patients in MASH clinical trials have shown significant benefit from monotherapy [55]. This phenomenon of reduced efficacy can be broadly considered a mechanism of drug resistance. Given that MAFLD is a complex, multifactorial disease with various mechanisms involved, it is unlikely that a single drug will effectively address all its aspects. In this context, thyroid hormone receptor beta (THRβ) agonists, FGF21 analogues, and glucagon-like peptide-1 receptor agonist (GLP-1Ras) exhibit varying degrees of therapeutic benefits for different pathological features of MAFLD and its related metabolic comorbidities [56], For example, FGF21 analogues and THRβ agonists appear to be more potent than GLP-1RAs in amelioration of hepatic steatosis, inflammation and fibrosis, but have minimal effects on obesity, insulin resistance and hyperglycaemia. In contrast, the amelioration in MAFLD by GLP-1RAs is accompanied by obvious improvement in weight loss and glycaemic control. Additionally, compensatory mechanisms might be involved in long-term drug treatment. For instance, Inhibition of ACLY, an enzyme involved in DNL, can be passed in the liver of mice fed a high-fructose diet [57] through upregulation of ACSS2. In addition, CYP4A could serve as a compensatory mechanism in the absence of CYP2E1 [58], which may lead to reduced efficacy in eliminating lipid peroxidation. Therefore, combination of agents might seem a logical approach to increase efficacy, with numerous combinations possible."

Limitations

Limitations of the present study include its design as a longitudinal trial without a placebo group. To address this limitation, we utilized baseline measurements as a control for comparison. Despite this, significant improvements in anti-inflammatory, anti-steatosis, and anti-fibrotic parameters were observed in patients receiving SNP-630-MS treatment compared to baseline. Another limitation of this study is the lack of liver biopsy results since histological evaluation plays an important role in the development of new drugs for MASH [59]. To achieve a breakthrough in the development of MASH therapeutic drugs, liver biopsies should be required in the trial design. Furthermore, lacking double-blind randomized protocol was also noted in the present study. Therefore, to further confirm the efficacy of SNP-630-MS, additional randomized placebo-controlled studies in patients with biopsy-proven MASH will be conducted in the future.

Conclusion

The findings of this study highlighted the potential of the novel SNP-630 and its metabolites in mitigating hepatic steatosis, MASH injury, and fibrosis through diverse mechanisms in a murine model of MASH. This study provides evidence for the efficacy and safety of SNP-630-MS, the active metabolites of SNP-630, in patients diagnosed with MASH and proposes SNP-630 and its active metabolites as promising candidates for the treatment of MASH. These finding are valuable for researchers aiming to understand pathophysiology and develop new therapies. Additionally, there is potential for the future availability of a unique oral therapy for MASH, which could be significant for patients, providers and caregivers seeking to prevent the progression and complications of this disease.

Abbreviations
MASH   Metabolic-associated steatohepatitis

Ho *et al. Journal of Translational Medicine*   (2024) 22:936

Page 16 of 18

SEM	Standard error
ALT	Alanine aminotransferase
IND	Investigational new drug
NASH	Non-alcoholic steatohepatitis
DNL	De novo lipogenesis
LPS	Lipopolysaccharides
ROS	Reactive oxygen species
CYP2E1	Cytochrome P450-2E1
FAS	Full analysis set
HFD	High-fat diet
ITT	Intention-to-treat
TG	Liver triglyceride
TCHO	Total cholesterol
IPs	Investigational products
H&E	Hematoxylin and eosin
TEAEs	Treatment-emergent adverse events
γ-GT	Gamma-glutamyl transpeptidase
PDFF	Proton density fat fraction
TLR4	Toll-like receptor 4
TNF-α	Tumor necrosis factor-alpha
IL-1β	Interleukin-1beta
T2DM	Type 2 diabetes

Supplementary Information

The online version contains supplementary material available at https://doi.org/10.1186/s12967-024-05686-7.

Additional file 1: SNP-630 and SNP-630-MS inhibit CYP2E1 protein expression in a mouse model of MASH. SNP-630-MS treatment significantly reduced CYP2E1 protein expression. Western blot analysis of CYP2E1 and β-actin was performed in mouse liver lysates. Body weight changes in mice fed an HFD. Serum monocyte chemoattractant protein 1 expression level. Serum CCL4 expression level. mRNA expression level of Col1a1. Data are expressed as mean ± SEM; n = 8 per group **$P < 0.01$ and ***$P < 0.005$ vs. HFD + vehicle group using a one-way analysis of variance followed by Fisher's least significant difference test comparing all groups to the HFD + vehicle group

Declarations

Ethics approval and consent to participate
The study was conducted in accordance with the principles of the Declaration of Helsinki and Good Clinical Practice guidelines from the International Conference on Harmonisation, and local applicable regulatory requirements. All procedures were approved by the institutional review boards/independent ethics committee at the leading site (Tri-Service General Hospital; IRB No.: 1-106-05-062). All patients provided written informed consent prior to screening. All animal husbandry, care, euthanasia, and use procedures followed the guidelines established by the Institutional Animal Care and Use Committees of the National Defense Medical Center (approval number: IACUC-15-309).

Consent for publication
Not applicable.

Competing interests
The authors declare that they have no competing interests.

Author details
[1]Sinew Pharma Inc. Rm C516, Building C, No.99, Lane 130, Sec. 1, Academia Rd., Nangang Dist, Taipei City 11571, Taiwan. [2]Division of Gastroenterology, Department of Internal Medicine, Tri-Service General Hospital, National Defense Medical Center, No. 325, Sec. 2, Chenggong Rd., Neihu District, Taipei 11420, Taiwan. [3]Division of Family and Community Health, Tri-Service General Hospital, National Defense Medical Center, Neihu Dist, Taipei 11420, Taiwan. [4]Division of Radiological Diagnosis, Tri-Service General Hospital, National Defense Medical Center, Neihu Dist, Taipei 11420, Taiwan. [5]Department of Medical Imaging, China Medical University Hsinchu Hospital and China Medical University, Hsinchu 302, Taiwan. [6]Institute of Nuclear Engineering and Science, National Tsing Hua University, Hsinchu 300, Taiwan. [7]School of Pharmacy, National Defense Medical Center, Neihu Dist, Taipei 11420, Taiwan. [8]Taipei Medical University, Taipei 110, Taiwan.

References
1. Powell EE, Wong VW, Rinella M. Non-alcoholic fatty liver disease. Lancet. 2021;397:2212–24. https://doi.org/10.1016/S0140-6736(20)32511-3.
2. Estes C, Razavi H, Loomba R, Younossi Z, Sanyal AJ. Modeling the epidemic of nonalcoholic fatty liver disease demonstrates an exponential increase in burden of disease. Hepatology. 2018;67:123–33. https://doi.org/10.1002/hep.29466.
3. Friedman SL, Neuschwander-Tetri BA, Rinella M, Sanyal AJ. Mechanisms of NAFLD development and therapeutic strategies. Nat Med. 2018;24:908–22. https://doi.org/10.1038/s41591-018-0104-9.
4. Raza S, Rajak S, Upadhyay A, Tewari A, Anthony SR. Current treatment paradigms and emerging therapies for NAFLD/NASH. Front Biosci. 2021;26:206–37. https://doi.org/10.2741/4892.
5. Sanjay KV, Vishwakarma S, Zope BR, Mane VS, Mohire S, Dhakshinamoorthy S. ATP citrate lyase inhibitor Bempedoic Acid alleviate long term HFD induced NASH through improvement in glycemic control, reduction of hepatic triglycerides & total cholesterol, modulation of inflammatory & fibrotic genes and improvement in NAS score. Curr Res Pharmacol Drug Discov. 2021;2: 100051. https://doi.org/10.1016/j.crphar.2021.100051.
6. Loomba R, Kayali Z, Noureddin M, Ruane P, Lawitz EJ, Bennett M, et al. GS-0976 reduces hepatic steatosis and fibrosis markers in patients with nonalcoholic fatty liver disease. Gastroenterology. 2018;155:1463-73.e6. https://doi.org/10.1053/j.gastro.2018.07.027.
7. Ratziu V, Sanyal A, Harrison SA, Wong VW, Francque S, Goodman Z, et al. Cenicriviroc treatment for adults with nonalcoholic steatohepatitis and fibrosis: final analysis of the phase 2b CENTAUR study. Hepatology. 2020;72:892–905. https://doi.org/10.1002/hep.31108.
8. Harrison SA, Wong VW, Okanoue T, Bzowej N, Vuppalanchi R, Younes Z, et al. Selonsertib for patients with bridging fibrosis or compensated

Ho *et al. Journal of Translational Medicine*   (2024) 22:936

Page 17 of 18

cirrhosis due to NASH: Results from randomized phase III STELLAR trials. J Hepatol. 2020;73:26–39. https://doi.org/10.1016/j.jhep.2020.02.027.

9. Harrison SA, Goodman Z, Jabbar A, Vemulapalli R, Younes ZH, Freilich B, et al. A randomized, placebo-controlled trial of emricasan in patients with NASH and F1–F3 fibrosis. J Hepatol. 2020;72:816–27. https://doi.org/10.1016/j.jhep.2019.11.024.

10. Carpi RZ, Barbalho SM, Sloan KP, Laurindo LF, Gonzaga HF, Grippa PC, et al. The effects of probiotics, prebiotics and Synbiotics in non-alcoholic fat liver disease (NAFLD) and non-alcoholic steatohepatitis (NASH): a systematic review. Int J Mol Sci. 2022;23:8805. https://doi.org/10.3390/ijms23158805.

11. Chen W, Yang A, Jia J, Popov YV, Schuppan D, You H. Lysyl oxidase (LOX) family members: rationale and their potential as therapeutic targets for liver fibrosis. Hepatology. 2020;72:729–41. https://doi.org/10.1002/hep.31236.

12. Sanyal AJ, Harrison SA, Ratziu V, Abdelmalek MF, Diehl AM, Caldwell S, et al. The natural history of advanced fibrosis due to nonalcoholic steatohepatitis: Data from the simtuzumab trials. Hepatology. 2019;70:1913–27. https://doi.org/10.1002/hep.30664.

13. Chalasani N, Abdelmalek MF, Garcia-Tsao G, Vuppalanchi R, Alkhouri N, Rinella M, et al. Effects of Belapectin, an inhibitor of galectin-3, in patients with nonalcoholic steatohepatitis with cirrhosis and portal hypertension. Gastroenterology. 2020;158:1334-1345.e5. https://doi.org/10.1053/j.gastro.2019.11.296.

14. Buzzetti E, Pinzani M, Tsochatzis EA. The multiple-hit pathogenesis of non-alcoholic fatty liver disease (NAFLD). Metabolism. 2016;65:1038–48. https://doi.org/10.1016/j.metabol.2015.12.012.

15. Suri J, Borja S, Lim JK. Combination strategies for pharmacologic treatment of non-alcoholic steatohepatitis. World J Gastroenterol. 2022;28:5129–40. https://doi.org/10.3748/wjg.v28.i35.5129.

16. Ratziu V, Charlton M. Rational combination therapy for NASH: insights from clinical trials and error. J Hepatol. 2023;78:1073–9. https://doi.org/10.1016/j.jhep.2022.12.025.

17. Chen Z, Tian R, She Z, Cai J, Li H. Role of oxidative stress in the pathogenesis of nonalcoholic fatty liver disease. Free Radic Biol Med. 2020;152:116–41. https://doi.org/10.1016/j.freeradbiomed.2020.02.025.

18. Ipsen DH, Lykkesfeldt J, Tveden-Nyborg P. Molecular mechanisms of hepatic lipid accumulation in non-alcoholic fatty liver disease. Cell Mol Life Sci. 2018;75:3313–27. https://doi.org/10.1007/s00018-018-2860-6.

19. Wang K, Tan W, Liu X, Deng L, Huang L, Wang X, et al. New insight and potential therapy for NAFLD: CYP2E1 and flavonoids. Biomed Pharmacother. 2021;137: 111326. https://doi.org/10.1016/j.biopha.2021.111326.

20. Harjumäki R, Pridgeon CS, Ingelman-Sundberg M. CYP2E1 in alcoholic and non-alcoholic liver injury roles of ROS, reactive intermediates and lipid overload. Int J Mol Sci. 2021. https://doi.org/10.3390/ijms22158221.

21. Abdelmegeed MA, Choi Y, Godlewski G, Ha SK, Banerjee A, Jang S, et al. Corrigendum: cytochrome P450–2E1 promotes fast food-mediated hepatic fibrosis. Sci Rep. 2017;7:42566. https://doi.org/10.1038/srep42566.

22. Abdelmegeed MA, Banerjee A, Yoo SH, Jang S, Gonzalez FJ, Song BJ. Critical role of cytochrome P450 2E1 (CYP2E1) in the development of high fat-induced non-alcoholic steatohepatitis. J Hepatol. 2012;57:860–6. https://doi.org/10.1016/j.jhep.2012.05.019.

23. Chalasani N, Gorski JC, Asghar MS, Asghar A, Foresman B, Hall SD, et al. Hepatic cytochrome P450 2E1 activity in nondiabetic patients with non-alcoholic steatohepatitis. Hepatology. 2003;37:544–50. https://doi.org/10.1053/jhep.2003.50095.

24. Kathirvel E, Chen P, Morgan K, French SW, Morgan TR. Oxidative stress and regulation of anti-oxidant enzymes in cytochrome P4502E1 transgenic mouse model of non-alcoholic fatty liver. J Gastroenterol Hepatol. 2010;25:1136–43. https://doi.org/10.1111/j.1440-1746.2009.06196.x.

25. Weltman MD, Farrell GC, Hall P, Ingelman-Sundberg M, Liddle C. Hepatic cytochrome P450 2E1 is increased in patients with nonalcoholic steatohepatitis. Hepatology. 1998;27:128–33. https://doi.org/10.1002/hep.510270121.

26. Jian T, Wu Y, Ding X, Lv H, Ma L, Zuo Y, et al. A novel sesquiterpene glycoside from Loquat leaf alleviates oleic acid-induced steatosis and oxidative stress in HepG2 cells. Biomed Pharmacother. 2018;97:1125–30. https://doi.org/10.1016/j.biopha.2017.11.043.

27. Frye RF, Adedoyin A, Mauro K, Matzke GR, Branch RA. Use of chlorzoxazone as an in vivo probe of cytochrome P450 2E1: choice of dose and

28. Pal P, Palui R, Ray S. Heterogeneity of non-alcoholic fatty liver disease: Implications for clinical practice and research activity. World J Hepatol. 2021;13:1584–610. https://doi.org/10.4254/wjh.v13.i11.1584.

29. Fraile JM, Palliyil S, Barelle C, Porter AJ, Kovaleva M. Non-alcoholic steatohepatitis (NASH)—a review of a crowded clinical landscape, driven by a complex disease. Drug Des Dev Ther. 2021;15:3997–4009. https://doi.org/10.2147/DDDT.S315724.

30. Dufour JF, Caussy C, Loomba R. Combination therapy for non-alcoholic steatohepatitis: rationale, opportunities and challenges. Gut. 2020;69:1877–84. https://doi.org/10.1136/gutjnl-2019-319104.

31. Alkhouri N, Herring R, Kabler H, Kayali Z, Hassanein T, Kohli A, et al. Safety and efficacy of combination therapy with semaglutide, cilofexor and firsocostat in patients with non-alcoholic steatohepatitis: a randomised, open-label phase II trial. J Hepatol. 2022;77:607–18. https://doi.org/10.1016/j.jhep.2022.04.003.

32. Smith GI, Shankaran M, Yoshino M, Schweitzer GG, Chondronikola M, Beals JW, et al. Insulin resistance drives hepatic de novo lipogenesis in nonalcoholic fatty liver disease. J Clin Invest. 2020;130:1453–60. https://doi.org/10.1172/JCI134165.

33. Ameer F, Scandiuzzi L, Hasnain S, Kalbacher H, Zaidi N. De novo lipogenesis in health and disease. Metabolism. 2014;63:895–902. https://doi.org/10.1016/j.metabol.2014.04.003.

34. Sanders FW, Griffin JL. De novo lipogenesis in the liver in health and disease: more than just a shunting yard for glucose. Biol Rev Camb Philos Soc. 2016;91:452–68. https://doi.org/10.1111/brv.12178.

35. Pawlak M, Lefebvre P, Staels B. Molecular mechanism of PPARα action and its impact on lipid metabolism, inflammation and fibrosis in non-alcoholic fatty liver disease. J Hepatol. 2015;62:720–33. https://doi.org/10.1016/j.jhep.2014.10.039.

36. Zhang Y, Yan T, Wang T, Liu X, Hamada K, Sun D, et al. Crosstalk between CYP2E1 and PPARα substrates and agonists modulate adipose browning and obesity. Acta Pharm Sin B. 2022;12:2224–38. https://doi.org/10.1016/j.apsb.2022.02.004.

37. Konstandi M, Cheng J, Gonzalez FJ. Sex steroid hormones regulate constitutive expression of Cyp2e1 in female mouse liver. Am J Physiol Endocrinol Metab. 2013;304:E1118–28. https://doi.org/10.1152/ajpendo.00585.2012.

38. Li H, Zhou Y, Wang H, Zhang M, Qiu P, Zhang M, et al. Crosstalk between liver macrophages and surrounding cells in nonalcoholic steatohepatitis. Front Immunol. 2020;11:1169. https://doi.org/10.3389/fimmu.2020.01169.

39. Cao Q, Mak KM, Lieber CS. Cytochrome P4502E1 primes macrophages to increase TNF-alpha production in response to lipopolysaccharide. Am J Physiol Gastrointest Liver Physiol. 2005;289:G95–107. https://doi.org/10.1152/ajpgi.00383.2004.

40. Ye Q, Wang X, Wang Q, Xia M, Zhu Y, Lian F, et al. Cytochrome P4502E1 inhibitor, chlormethiazole, decreases lipopolysaccharide-induced inflammation in rat Kupffer cells with ethanol treatment. Hepatol Res. 2013;43:1115–23. https://doi.org/10.1111/hepr.12063.

41. Zhou Y, Zhang H, Yao Y, Zhang X, Guan Y, Zheng F. CD4+ T cell activation and inflammation in NASH-related fibrosis. Front Immunol. 2022;13: 967410. https://doi.org/10.3389/fimmu.2022.967410.

42. Ramadori P, Kam S, Heikenwalder M. T cells: friends and foes in NASH pathogenesis and hepatocarcinogenesis. Hepatology. 2022;75:1038–49. https://doi.org/10.1002/hep.32336.

43. Dudek M, Pfister D, Donakonda S, Filpe P, Schneider A, Laschinger M, et al. Auto-aggressive CXCR6+ CD8 T cells cause liver immune pathology in NASH. Nature. 2021;592:444–9. https://doi.org/10.1038/s41586-021-03233-8.

44. Woestemeier A, Scognamiglio P, Zhao Y, Wagner J, Muscate F, Casar C, et al. Multicytokine-producing CD4+ T cells characterize the livers of patients with NASH. JCI Insight. 2023;8: e153831. https://doi.org/10.1172/jci.insight.153831.

45. Haas JT, Vonghia L, Mogilenko DA, Verrijken A, Molendi-Coste O, Fleury S, et al. Author correction: transcriptional network analysis implicates altered hepatic immune function in NASH development and resolution. Nat Metab. 2019;1:744. https://doi.org/10.1038/s42255-019-0093-0.

46. Rau M, Schilling AK, Meertens J, Hering I, Weiss J, Jurowich C, et al. Progression from nonalcoholic fatty liver to nonalcoholic steatohepatitis is marked by a higher frequency of Th17 cells in the liver and an increased

Ho *et al. Journal of Translational Medicine*   (2024) 22:936

Page 18 of 18

Th17/resting regulatory T cell ratio in peripheral blood and in the liver. J Immunol. 2016;196:97–105. https://doi.org/10.4049/jimmunol.1501175.

47. Zani F, Blagih J, Gruber T, Buck MD, Jones N, Hennequart M, et al. The dietary sweetener sucralose is a negative modulator of T cell-mediated responses. Nature. 2023;615:705–11. https://doi.org/10.1038/s41586-023-05801-6.

48. Jeon HJ, Choi DK, Choi J, Lee S, Lee H, Yu JH, et al. D-mannitol induces a brown fat-like phenotype via a β3-adrenergic receptor-dependent mechanism. Cells. 2021;10:768. https://doi.org/10.3390/cells10040768.

49. Rinella ME, Dufour JF, Anstee QM, Goodman Z, Younossi Z, Harrison SA, et al. Non-invasive evaluation of response to obeticholic acid in patients with NASH: results from the regenerate study. J Hepatol. 2022;76:536–48. https://doi.org/10.1016/j.jhep.2021.10.029.

50. Harrison SA, Bashir MR, Guy CD, Zhou R, Moylan CA, Frias JP, et al. Resmetirom (MGL-3196) for the treatment of non-alcoholic steatohepatitis: a multicentre, randomised, double-blind, placebo-controlled, phase 2 trial. Lancet. 2019;394:2012–24. https://doi.org/10.1016/S0140-6736(19)32517-6.

51. Eslam M, George J. Genetic contributions to NAFLD: leveraging shared genetics to uncover systems biology. Nat Rev Gastroenterol Hepatol. 2020;17:40–52. https://doi.org/10.1038/s41575-019-0212-0.

52. Wang JZ, Cao HX, Chen JN, Pan Q. PNPLA3 rs738409 underlies treatment response in nonalcoholic fatty liver disease. World J Clin Cases. 2018;6:167–75. https://doi.org/10.12998/wjcc.v6.i8.167.

53. Dallio M, Masarone M, Romeo M, Tuccillo C, Morisco F, Persico M, et al. PNPLA3, TM6SF2, and MBOAT7 influence on nutraceutical therapy response for non-alcoholic fatty liver disease: a randomized controlled trial. Front Med. 2021;8: 734847. https://doi.org/10.3389/fmed.2021.734847.

54. Marra F, Tacke F. Roles for chemokines in liver disease. Gastroenterology. 2014;147:577-94.e1. https://doi.org/10.1053/j.gastro.2014.06.043.

55. Dufour JF, Caussy C, Loomba R. Combination therapy for non-alcoholic steatohepatitis: rationale, opportunities and challenges. Gut. 2020;69(10):1877–84. https://doi.org/10.1136/gutjnl-2019-319104.

56. Chui ZSW, Xue Y, Xu A. Hormone-based pharmacotherapy for metabolic dysfunction-associated fatty liver disease. Med Rev. 2024;4(2):158–68. https://doi.org/10.1515/mr-2024-0007.

57. Zhao S, Jang C, Liu J, Uehara K, Gilbert M, Izzo L, et al. Dietary fructose feeds hepatic lipogenesis via microbiota-derived acetate. Nature. 2020;579(7800):586–91. https://doi.org/10.1038/s41586-020-2101-7.

58. Leclercq IA, Farrell GC, Field J, Bell DR, Gonzalez FJ, Robertson GR. CYP2E1 and CYP4A as microsomal catalysts of lipid peroxides in murine nonalcoholic steatohepatitis. J Clin Investig. 2000;105:1067–75. https://doi.org/10.1172/JCI8814.

59. Tong XF, Wang QY, Zhao XY, Sun YM, Wu XN, Yang LL, et al. Histological assessment based on liver biopsy: the value and challenges in NASH drug development. Acta Pharmacol Sin. 2022;43:1200–9. https://doi.org/10.1038/s41401-022-00874-x.

Publisher's Note